JCB Article

Visualization of Rab9-mediated vesicle transport from endosomes to the trans-Golgi in living cells

Pierre Barbero, Lenka Bittova, and Suzanne R. Pfeffer

Department of Biochemistry, Stanford University School of Medicine, Stanford, CA 94305

Mannose 6-phosphate receptors (MPRs) are transported from endosomes to the trans-Golgi via a transport process that requires the Rab9 GTPase and the cargo adaptor TIP47. We have generated green fluorescent protein variants of Rab9 and determined their localization in cultured cells. Rab9 is localized primarily in late endosomes and is readily distinguished from the trans-Golgi marker galactosyltransferase. Coexpression of fluorescent Rab9 and Rab7 revealed that these two late endosome Rabs occupy distinct domains within late endosome membranes. Cation-independent mannose 6-phosphate receptors are enriched in the Rab9 domain relative to the Rab7 domain. TIP47 is likely to be present in this domain because it colocalizes with the receptors in fixed cells, and a TIP47 mutant disrupted endosome morphology and sequestered MPRs intracellularly. Rab9 is present on endosomes that display bidirectional microtubule-dependent motility. Rab9-positive transport vesicles fuse with the trans-Golgi network as followed by video microscopy of live cells. These data provide the first indication that Rab9-mediated endosome to trans-Golgi transport can use a vesicle (rather than a tubular) intermediate. Our data suggest that Rab9 remains vesicle associated until docking with the Golgi complex and is rapidly removed concomitant with or just after membrane fusion.

Introduction

Mannose 6-phosphate receptors (MPRs)* carry newly synthesized lysosomal enzymes from the Golgi to prelysosomes and then return to the Golgi complex to reinitiate an enzyme delivery cycle (Kornfeld, 1992). We study the return step: the transport of MPRs from late endosomes to the trans-Golgi. We have shown that this step requires the Rab9 GTPase (Lombardi et al., 1993; Riederer et al., 1994), the cargo adaptor, TIP47 (Diaz and Pfeffer, 1998; Carroll et al., 2001), a Rab9 effector named p40 (Diaz et al., 1997), NSF, α-SNAP, and a protein named mapmodulin (Itin et al., 1997, 1999).

TIP47 binds with high specificity to the cytosolic domains of the cation-dependent and cation-independent MPRs (Diaz and Pfeffer, 1998). Indeed, TIP47 fails to bind to other proteins that are transported from late endosomes to the Golgi complex including furin, carboxypeptidase D, TGN38, and the HIV Nef protein (Krise et al., 2000). TIP47 recognizes a Phe-Trp motif in the CD-MPR (Diaz and Pfeffer, 1998) and a proline-rich region of the CI-MPR (Orsel et al., 2000). We have shown recently that TIP47 also binds directly to Rab9 (Carroll et al., 2001). TIP47 can bind to Rab9 and MPRs simultaneously via physically distinct domains. Moreover, Rab9 increases the affinity of TIP47 for MPR cytoplasmic domains (Carroll et al., 2001). In this way, it appears that Rab9 facilitates the process of MPR cargo collection during the process of transport vesicle formation.

But what are the transport carriers that deliver MPRs from late endosomes to the Golgi complex? Function blocking anticlathrin antibodies failed to inhibit MPR recycling to the trans-Golgi under conditions in which they strongly interfered with transferrin endocytosis (Draper et al., 1990). Thus, it appears that clathrin may not play a role in MPR recycling. TIP47 may replace clathrin in this step because it occurs as a large oligomer in cytosol, and it may have the capacity to bind cargo and to function as a coat protein.

We report here experiments designed to visualize MPR trafficking in live cells. Although to date we have been unable to generate a functional fluorescent TIP47 protein, we succeeded in monitoring green fluorescent protein (GFP) variants of Rab9 by video microscopy. We describe here the morphology and motility of organelles and transport vesicles

The online version of this article contains supplemental material.

Address correspondence to Suzanne R. Pfeffer, Dept. of Biochemistry, B400, Stanford University School of Medicine, Stanford, CA 94305-5307. Tel.: (650) 723-6169. Fax: (650) 723-6783. E-mail: pfeffer@cmgm.stanford.edu

*Abbreviations used in this paper: CFP, cyan fluorescent protein; GFP, green fluorescent protein; MPR, mannose 6-phosphate receptor; TGN, trans-Golgi network; YFP, yellow fluorescent protein.

Key words: endosome; Rab9; Golgi complex; Rab7; TIP47

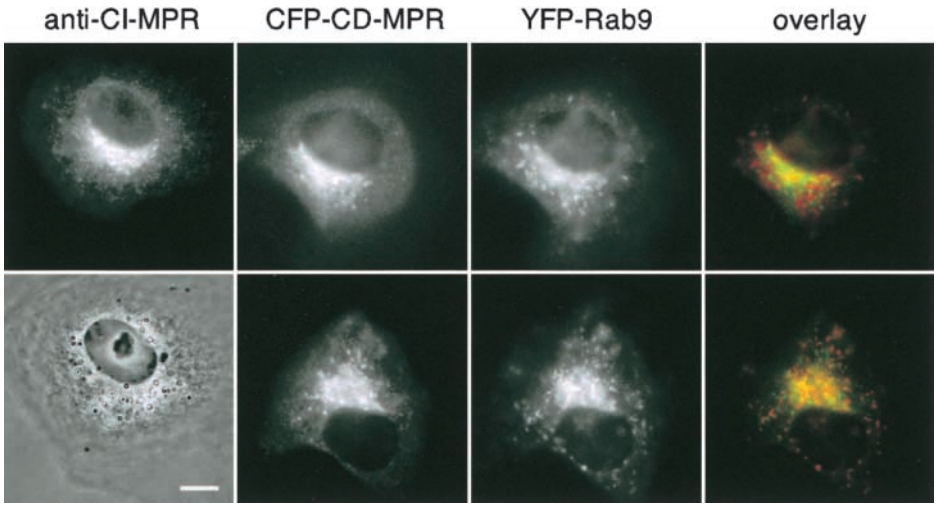

Figure 1. **Localization of fluorescent Rab9protein in living cells.** BS-C-1 cells expressing CFP-CD-MPR and YFP-Rab9 (second, third, and fourth columns) were analyzed by fluorescence microscopy in comparison with untransfected fixed cells (first column). Endogenous CI-MPRs were detected using mouse anti–CI-MPR culture supernatant. The overlays at right show CFP-CD-MPR (green), YFP-Rab9 (red), and colocalization of both proteins (yellow). Bar, 10 μm.

that carry Rab9 on their surfaces. We also describe distinct domains occupied by two late endosomal Rab GTPases: Rab9 and Rab7.

Results

We have shown previously that Rab9 colocalizes significantly with the CI-MPR, primarily in late endosomes but to a small extent in the Golgi complex and displays a punctate perinuclear "half moon" pattern in fixed cells (Lombardi et al., 1993). A construct comprised of yellow fluorescent protein (YFP) fused to the NH_2 terminus of Rab9 (YFP-Rab9) was also present mostly in late endosomes in living cells (Fig. 1). The overlap was less extensive with the cyan fluorescent protein (CFP)-tagged CD-MPR than that seen previously with the CI-MPR. This could be due to the possibility that much of the CFP-CD-MPR resides in the trans-Golgi network (TGN) as reported by Bonifacino and colleagues (Puertollano et al., 2001), whereas Rab9 and CI-MPR are predominantly in late endosomes. It is possible that the CFP tag at the COOH terminus of the CD-MPR alters its rate of export from the TGN.

The YFP-Rab9 staining seemed to include structures located further away from the nucleus than those that housed the CD-MPR in live cells or the CI-MPR in fixed cells (Fig. 1). YFP-Rab9–labeled structures were not positive for the trans-Golgi marker galactosyltransferase (see Fig. 8). In addition, they were essentially all positive for endocytosed dextran (unpublished data), confirming that YFP-Rab9 had a primarily endosomal localization.

Membrane association of Rab9 requires that Rab9 be prenylated. Significant membrane association of the GFP-Rab9 was confirmed by analyzing cell extracts by sucrose density gradient flotation (Fig. 2). Transfected cells were harvested, and the extract was underlaid at the bottom of a sucrose gradient. After centrifugation, the gradient fractions were ana-

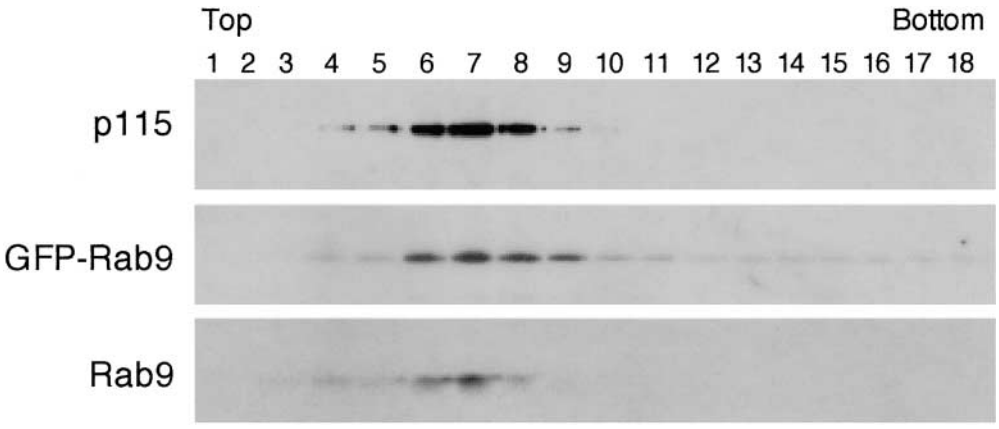

Figure 2. **GFP-Rab9 distribution in BS-C-1 cell extracts subjected to sucrose density gradient flotation.** Fractions were collected from the top (fraction 1) to the bottom (fraction 18) of the gradient. Aliquots of each fraction were analyzed by immunoblot using anti-p115 (top) or anti-Rab9 culture supernatant (middle and bottom).

lyzed by immunoblot. Golgi membranes, as monitored by the distribution of the protein p115, were found in a band collected in fractions 5–9 of the gradient (Fig. 2); endosomes cofractionate with Golgi membranes under these conditions (Diaz and Pfeffer, 1998). Both the GFP-Rab9 and endogenous Rab9 protein floated to this region of the gradient. In addition, we detected nonmembrane-associated GFP-Rab9 that trailed from the fractions containing the initial homogenate at the bottom of the gradient (fractions 9–18; Fig. 2). This experiment confirms that most of the GFP-Rab9 becomes membrane associated and cofractionates with endogenous Rab9 protein. Nevertheless, GFP-Rab9 was less efficiently delivered to membranes than wild-type Rab9 protein. GFP-Rab9 bound guanine nucleotides (unpublished data), which would be a requirement for its functionality. The less efficient membrane association could have been due to differences in prenylation efficiency and/or differences in interaction with modulators and effectors that mediate membrane association because of the presence of the GFP.

Rab9 and Rab7 define distinct domains

Zerial and coworkers have shown that early endosomal Rabs define distinct membrane domains within a single membrane-bound organelle. Thus, Rab5 and Rab4 are segregated within early endosomes and are likely to associate with distinct effectors retained in these domains by interaction with the respective Rab proteins (Sonnichsen et al., 2000; Zerial and McBride, 2001). Therefore, we were interested to investigate whether two late endosomal Rabs, Rab7 and Rab9, also displayed membrane domain segregation.

Expression of YFP-Rab9 and CFP-Rab7 in BS-C-1 cells revealed a very similar pattern of protein localization (Fig. 3, top), but remarkably the proteins were present in distinct regions. As seen before for GFP-Rab7 (Bucci et al., 2000), Rab7 was detected in perinuclear late endosomes. As shown in video 1 available at http://www.jcb.org/cgi/content/full/jcb.200109030/DC1 and Fig. 3 (bottom right), Rab7 and Rab9 were often associated with what appeared to be a single organelle that rotated and translated along microtubules without displaying significant mixing of the two GTPases. The red and green labels resembled two macaroon cookies sandwiched together. In addition, some organelles were positive for Rab7 or Rab9 but not both GTPases. Occasionally, a rim of overlap could be detected between the two domains. Thus, Rab7 and Rab9 appear to define distinct endosomal domains and are not always present on the same endosome.

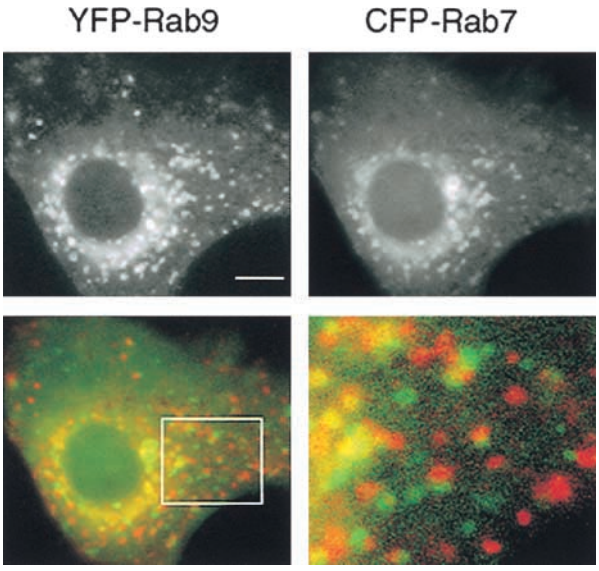

Figure 3. **YFP-Rab9 and CFP-Rab7 localize to distinct domains on late endosomes.** See also video 1 available at http://www.jcb.org/cgi/content/full/jcb.200109030/DC1. YFP-Rab9 (top left) and CFP-Rab7 (top right) in living transfected BS-C-1 cells. Overlay of both images (bottom) shows CFP-Rab7 (green), YFP-Rab9 (red), and the colocalization of both proteins (yellow). The box in the overlay indicates the boundaries of the enlarged image shown in the bottom right panel. Bar, 10 μm.

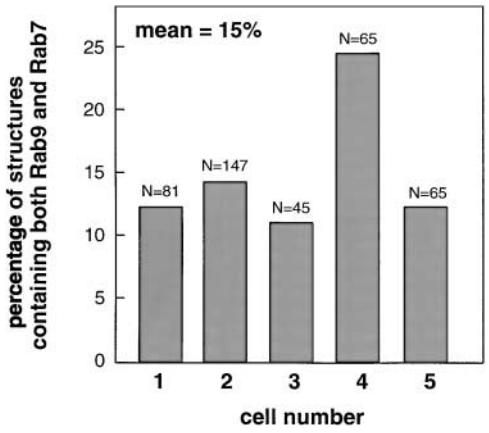

Figure 4. **Quantitation of the overlap between Rab9 and Rab7.** Cells were transfected with plasmids encoding YFP-Rab9 and CFP-Rab7. Labeled structures containing Rab9, Rab7, or both were counted at high magnification on a computer screen using Metamorph software. Total number of structures counted (N) is shown for five different cells.

Quantitation of >400 Rab9- and Rab7-positive structures in five cells expressing both constructs revealed that only 15% of the Rab9 or Rab7 labeling overlapped. In other words, in 85% of the structures scored Rab9 and Rab7 occupied distinct domains (Fig. 4).

CI-MPRs are concentrated in Rab9-enriched endosome domains

If Rab9 and Rab7 domains are functionally distinct, MPRs might be enriched in membranes containing Rab9 protein. To test this, we used a monoclonal antibody that recognizes the lumenal domain of the CI-MPR and labeled it directly by conjugation with Texas red. We then incubated cells with this reagent for 3 h to label MPRs. At least in CHO cells, CI-MPRs appear at the cell surface once every 3 h as part of their normal intracellular cycling (Sahagian and Neufeld, 1983). Moreover, the antibody we employed remains receptor bound above pH 3.0 (unpublished data), and therefore should remain receptor bound in early and late endosomes.

Under certain conditions, polyclonal antibodies can trigger receptor delivery to lysosomes, but a huge excess of antibody is required: for example, addition of 10% polyclonal anti–CI-MPR antiserum for 5 h decreased receptor levels by 30% (Pfeffer, 1987). We instead added

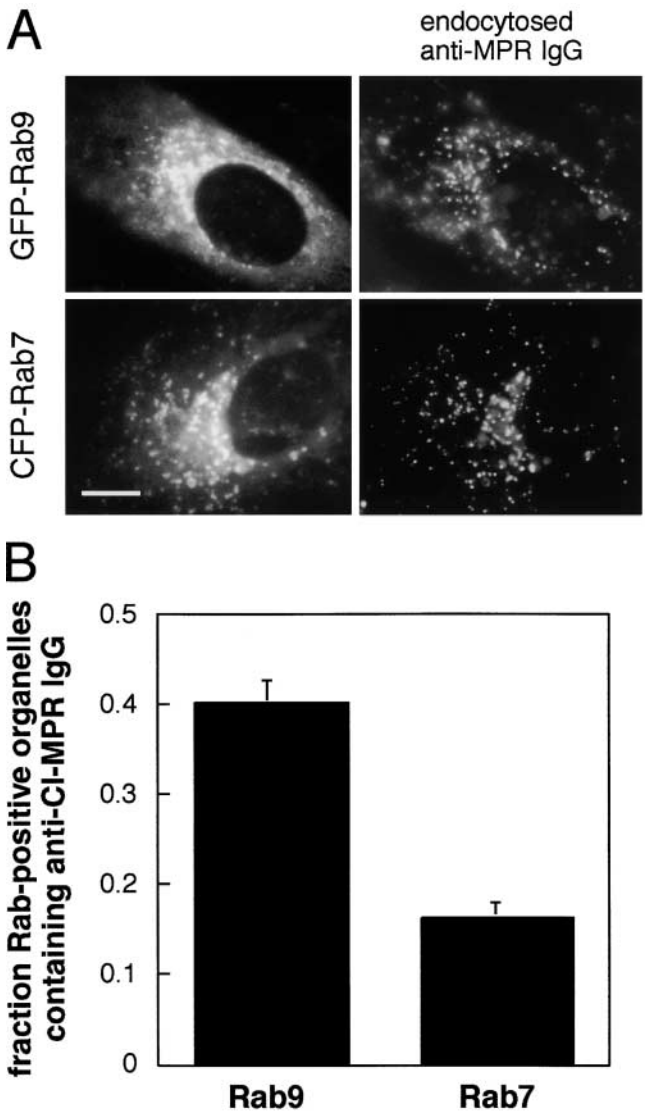

Figure 5. **Distribution of the CI-MPR in Rab9 and Rab7 endosomal subdomains.** Cells expressing either GFP-Rab9 or CFP-Rab7 were incubated with Texas red anti–CI-MPR for 3 h and chased for 15 min at 37°C to label a large fraction of total cellular CI-MPRs as shown in A. The proportion of Rab9- or Rab7-positive structures that contained anti–CI-MPR IgG was quantified using Metamorph software on a large computer screen (B). For Rab9, 370 total structures were counted from 8 cells; 146 of these contained anti-MPR IgG. For Rab7, 1,529 vesicles were counted from 15 cells; 250 of these contained MPR IgG. Standard error of the mean was determined using the values obtained for each individual cell analyzed.

monoclonal anti–CI-MPR IgG for 3 h at 20 μg/ml antibody, which did not seem to alter MPR trafficking (see below).

As shown in Fig. 5 A, fluorescent anti–CI-MPR IgG was present in punctate structures throughout the cytoplasm that resembled early and late endosomes as expected. To determine the distribution of MPR IgG within late endosomes, we scored all Rab9- or Rab7-positive structures and then determined the percentage of those membrane domains that also housed anti–CI-MPR IgG. Although 16% of Rab7-positive domains also contained anti-MPR IgG (n = 1,529), 40% of Rab9-positive domains were doubly positive for anti-MPR IgG (n = 370) (Fig. 5 B). These data show that CI-MPRs are enriched in Rab9-positive regions of late endosomes. Because it is unlikely that every molecule of CI-MPR will have an antibody molecule attached to it, our values are likely to represent an underestimate of the fraction of Rab9 domains that actually contain MPRs. In addition, our antibody labeling protocol will include MPRs en route to the late endosome from the cell surface. Thus, it is possible that MPRs in the Rab7 domain may be en route to the Rab9 domain.

What molecules might enrich MPRs within the Rab9 domain? TIP47 is likely to link Rab9 and MPRs into a common endosomal subdomain. Unfortunately, we do not yet have a functional GFP-TIP47 to test this directly. However, we have generated a mutant of TIP47 that binds MPRs with wild-type affinity but is severely diminished in its ability to bind Rab9 (Carroll et al., 2001). Expression of this mutant protein inhibits the transport of MPRs from endosomes to the trans-Golgi in living cells (Carroll et al., 2001).

If TIP47 is required for Rab9 domain generation, expression of the mutant protein might generate aberrant endosomal structures by forming a nonfunctional Rab9-MPR-TIP47 assembly. To test this possibility, cells stably expressing YFP-Rab9 were transiently transfected with two plasmids: one encoding CFP to permit detection of transfected cells and a second plasmid encoding TIP47$^{SVV\text{-}AAA}$ (Carroll et al., 2001).

As shown in Fig. 6 A, expression of TIP47$^{SVV\text{-}AAA}$ often yielded significantly larger and unusual looking Rab9-positive structures (bottom) than seen in cells that did not express the mutant protein (top). In addition, cells expressing the TIP47 mutant protein endocytosed significantly less anti-MPR IgG (Fig. 6 B, middle compared with bottom or control panel at the top). This suggests that TIP47$^{SVV\text{-}AAA}$ has sequestered MPRs intracellularly, blocking both their recycling to the TGN (Carroll et al., 2001) and their ability to cycle via the plasma membrane. TIP47 has been shown already to colocalize with MPRs in fixed cells (Diaz and Pfeffer, 1998) and is present in late endosomes in mutant TIP47-expressing cells (unpublished data). Because the TIP47 mutant can influence the appearance of Rab9-positive compartments and sequester MPRs intracellularly, the simplest explanation would be that TIP47 is part of the Rab9- and MPR-enriched endosomal subdomain.

Rab9 vesicles en route to the trans-Golgi

The major goal of this project was to visualize Rab9 vesicles en route from endosomes to the trans-Golgi, since such transport intermediates had never before been detected. This question was complicated by the fact that endosomes and the Golgi are found directly adjacent to each other in the perinuclear region of the cell. Thus, distinguishing rare transport vesicles in this crowded region of the cytoplasm is challenging.

We took two approaches to circumvent this problem. First, we treated cells with nocodazole to depolymerize microtubules and disperse both endosomes and the Golgi complex (Fig. 7 A). We have shown that endosome to trans-Golgi transport of MPRs does not require intact microtubules; intact microtubules enhance the initial rate

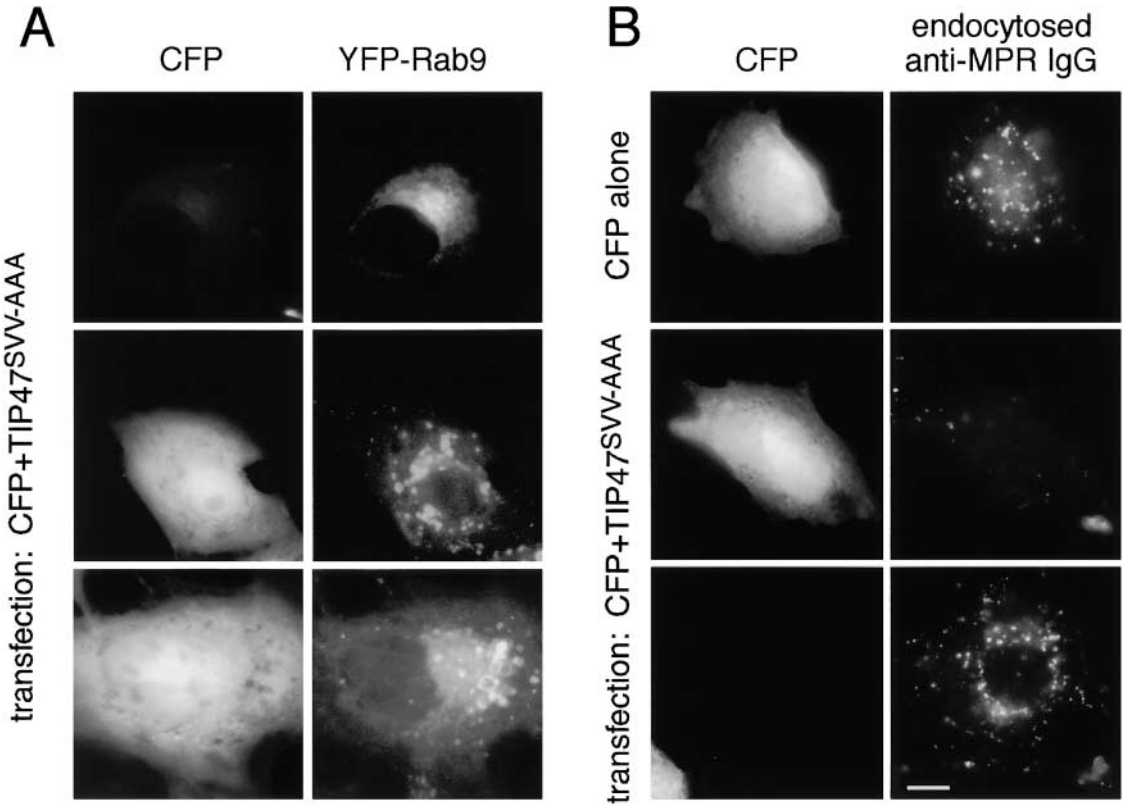

Figure 6. **A TIP47 mutant disrupts the Rab9 compartment and sequesters MPRs intracellularly.** (A) Cells stably expressing YFP-Rab9 were transiently cotransfected with plasmids encoding CFP (to detect transfected cells, left column) and TIP47$^{SVV\text{-}AAA}$. The distribution of Rab9 (right column) was visualized by light microscopy. (B) BS-C-1 cells were transfected with a plasmid encoding either CFP alone (top row) or CFP and TIP47$^{SVV\text{-}AAA}$. Cells were then incubated with Texas red anti–CI-MPR at 37°C as in Fig. 5.

but not the overall extent of transport (Itin et al., 1999). In the absence of nocodazole, vesicles moved with a velocity of ~0.75 μm/s; upon microtubule depolymerization, this decreased to ~0.2 μm/s (Fig. 7 B). Motility was bidirectional (video 2 available at http://www.jcb.org/cgi/content/full/jcb.200109030/DC1). Despite the loss of most high velocity motility in nocodazole-treated cells, some residual microtubules were seen as were Rab9-positive vesicles moving along them (video 3 available at http://www.jcb.org/cgi/content/full/jcb.200109030/DC1).

Shown in Fig. 7 A and in video 3 available at http://www.jcb.org/cgi/content/full/jcb.200109030/DC1 is a set of time-lapse images that reveals a vesicle moving from one Rab9-positive compartment to another. Note that transfer is

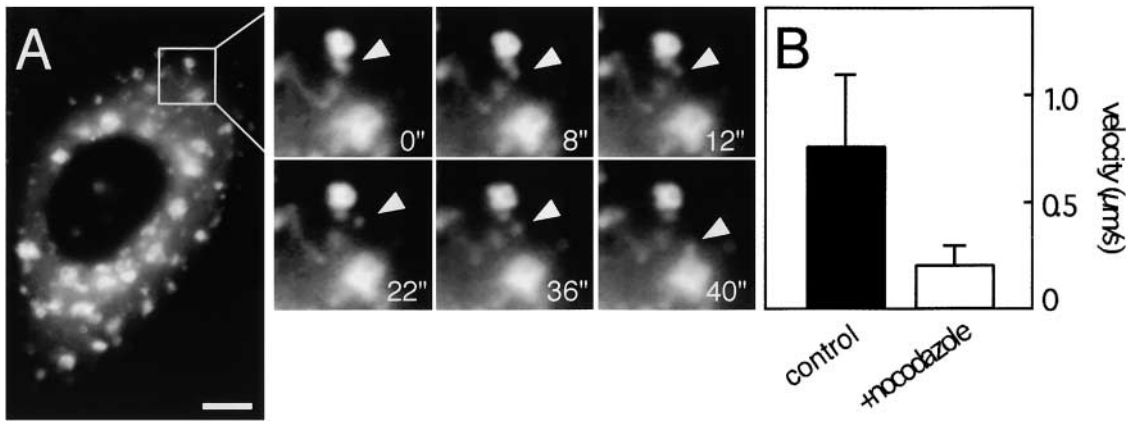

Figure 7. **GFP-Rab9–bearing vesicles display microtubule-based motility.** See also videos 2 and 3 available at http://www.jcb.org/cgi/content/full/jcb.200109030/DC1. BS-C-1 cells transfected with pEGFP-Rab9 were treated with or without 4 μg/ml nocodazole for 1 h at 37°C and analyzed by time-lapse video microscopy at 37°C. (A) GFP-Rab9 localization in BS-C-1 nocodazole-treated cells and enlarged selected video images from a time-lapse series. The white arrowhead points to a GFP-Rab9–bearing vesicle. (B) GFP-Rab9 vesicle velocity in BS-C-1–transfected cells with (+ nocodazole) or without (control). Bar, 5 μm.

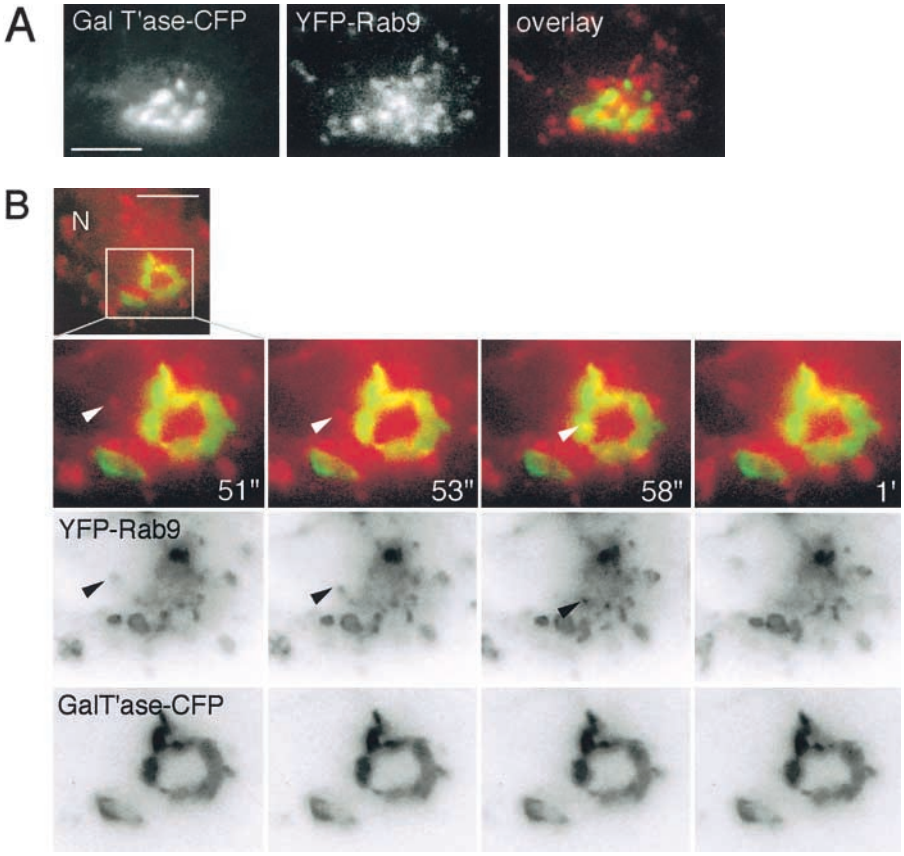

Figure 8. **Visualization of a Rab9-bearing vesicle fusing with the trans-Golgi detected by time-lapse video microscopy.** See also video 4 available at http://www.jcb.org/cgi/content/full/jcb.200109030/DC1. BS-C-1 cells transfected with pECFP-galactosyltransferase (GalT′ase) and pEYFP-Rab9 were analyzed by fluorescence microscopy. (A) GalT′ase-CFP (left) and YFP-Rab9 (middle) in transfected cells. Overlay of GalT′ase-CFP (green) and YFP-Rab9 (red) is shown on the right. (B) Enlarged selected video images from a time-lapse series of BS-C-1 cells expressing GalT′ase-CFP and YFP-Rab9 proteins. Overlay images (top row) shows GalT′ase-CFP (green), YFP-Rab9 (red), and colocalization at docking and possibly fusion (yellow). Overlay images were obtained by overlapping GalT′ase-CFP signal (middle row) and YFP-Rab9 signal (bottom row). N, nucleus. Bars, 10 μm.

accomplished by a vesicle rather than a tubule. But what are these compartments that are mixing by vesicular transfer? To better determine the identity of the acceptor compartment, we used the trans-Golgi marker CFP–galactosyltransferase.

The CFP–galactosyltransferase construct employed contains 81 NH_2-terminal amino acids of human β 1,4-galactosyltransferase, including the membrane-anchoring peptide that targets the fusion protein to the trans- and medial-Golgi (Llopis et al., 1998). Upon expression in BS-C-1 cells, this chimeric construct is also found in the trans-Golgi network because it could be shown to overlap with AP-1 at the TGN (unpublished data). Using immunogold EM, Llopis et al. (1998) reported colocalization of this fluorescent galactosyltransferase construct with the TGN marker, TGN38. This is important, because it has been shown previously that MPRs recycle to sialyltransferase-positive compartments (TGN) but not galactosyltransferase-positive compartments (trans-Golgi) of CHO cells (Duncan and Kornfeld, 1988).

CFP-galactosyltransferase–positive structures were distinct from YFP-Rab9 structures upon cotransfection of BS-C-1 cells (Fig. 8 A). This confirms our earlier conclusion that most of the Rab9 is present on late endosomes; a small amount may be on the TGN.

Close examination of these cells by video microscopy revealed vesicle transfers from Rab9-positive compartments to the trans-Golgi (Fig. 8 B; video 4 available http://www.jcb.org/cgi/content/full/jcb.200109030/DC1). The time-lapse series shown in the video reveals two successive vesicle-sized intermediates that appear to be fusing directly with what can be defined as the Golgi by virtue of its content of a bona fide Golgi marker. Both of the vesicles follow an identical approach pathway, which is likely provided by an unlabeled microtubule. Thus, these images capture the transfer of Rab9 vesicles from what is likely to represent a late endosome to the Golgi complex in real time. In addition, the data support the proposal that Rab9 remains vesicle associated throughout vesicle budding, docking, and less clear but possibly also, fusion events. The loss of red color from the Golgi just before or after fusion could be due to GDI-mediated removal of Rab9 from that compartment or alternatively could reflect Rab9 dilution in the target membrane bilayer. Indeed, the rapid loss of Rab9 staining on the target membrane was impressive.

Discussion

Unlike the transport of proteins from the ER to the Golgi or from the Golgi to the plasma membrane, the transport of MPRs from endosomes to the trans-Golgi is a relatively low volume process. For example, the ER-to-Golgi Rab1B GTPase is 40 times more abundant in mammalian cells than Rab9 (Soldati et al., 1995), and that pathway may involve 40 times as many transport vesicles. The low volume of endosome to trans-Golgi transport together with the low abundance of the requisite molecular machinery have hindered detection of transport intermediates in previous studies. Although MPRs have been documented as cargo of clathrin-coated vesicles that leave the TGN en route to prelysosomal compartments (Klumperman et al., 1993), little is known about the pathway that carries MPRs back to the Golgi.

We have shown for the first time that Rab9 is present on vesicles that bud off of Rab9-positive structures. In addition, small Rab9-positive vesicles can fuse with the Golgi complex. We do not yet know what proteins coat these vesicles, but a prediction of our model is that they bear TIP47 on their surfaces. In addition, Rab9 remains vesicle associated at least through the docking reaction and possibly until after the fusion process is complete.

We have shown that like early endosomal Rabs Rab9 occupies a discrete domain on late endosome membranes that include MPRs and is likely to also include other proteins needed for vesicle formation, docking, and fusion. Rab7 was generally adjacent to Rab9, although some vesicles were positive for one of the two Rabs and not the other. Because the two domains were so distinct, it remains possible that we are visualizing two discrete vesicles that are tightly attached to each other. However, their remarkably close association seen by video microscopy appeared more consistent with the Rabs occupying distinct domains in a single membrane-bound compartment. In either case, the Rabs define distinct membrane domains.

TIP47 is likely to enrich MPRs within the Rab9 domain. In support of this conclusion is our finding that a mutant TIP47 that binds poorly to Rab9 alters dramatically the appearance of Rab9-positive compartments. Our working model is that the mutant protein coassembles with native TIP47 to form an aberrant structure. In other work, we have shown that a myc-tagged TIP47 coassembles with endogenous wild-type TIP47. Such coassembled mutant complexes may sequester MPRs within late endosomes; indeed, cells expressing the TIP47 mutant endocytosed significantly less anti–MPR-IgG than control cells and showed altered morphology of Rab9-positive compartments. Altogether, these data suggest that TIP47, Rab9, and MPRs are present altogether in an endosomal subdomain.

Do the transport vesicles we have visualized contain MPRs? MPR transport from endosomes to the Golgi complex is completely dependent on Rab9 function (Lombardi et al., 1993; Riederer et al., 1994). In addition, we have shown here that Rab9 domains from which the vesicles bud are enriched in CI-MPRs. Unfortunately, we could not get enough label onto MPRs to detect their presence in nascent vesicles containing Rab9 protein. In addition, little of the CFP-CD-MPR is ever seen in late endosomes at steady-state, making it unusable as a cargo marker for the retrograde transport route. It seems very possible that the CFP on the cytoplasmic domain of the CD-MPR may slow the export of this receptor from the TGN.

Although some vesicles might be formed that do not contain MPRs, the simplest model is that MPRs are indeed contained within the Rab9-positive vesicles. Because Rab9 enhances the affinity of TIP47 for MPR cytoplasmic domains, it seems reasonable to propose that these proteins are packaged altogether into transport carriers. In any event, we never saw tubules emerge from the Rab9 domain nor did we detect CI-MPRs in tubules emerging from Rab9-positive structures.

Rab7 is believed to function in the homotypic fusion of late endosomes (Feng et al., 1995; Bucci et al., 2000). This is distinct from the function of Rab9, which is needed for MPR recycling to the Golgi complex (Lombardi et al., 1993; Riederer et al., 1994). It will be of interest to determine if organelles positive for Rab9 or Rab7 (but not both) are capable of fusing with each other. If, like Rab5 in early endosomes, Rab7 organizes the homotypic late endosome fusion machinery, it is possible that the $Rab9^+$ $Rab7^-$ organelles will have lost the capacity to fuse at high efficiency with the $Rab7^+$ $Rab9^-$ organelles. Our experiments cannot rule out the presence of nonfluorescent Rab7 in a Rab9-positive compartment. Yet the observations suggest an unappreciated possibility that formation of a Rab9-positive Rab7-negative organelle would yield a terminal compartment that can no longer fuse with other late endosomes; it would only retain the capacity to bud off Rab9 vesicles or be a target for autophagic consumption. Therefore, late endosomes may have a mechanism to retain Rab7 and Rab9 in distinct domains within a single membrane-bound organelle to avoid such an outcome.

We have tried to construct functional fluorescent TIP47 chimeras using GFP, YFP, and CFP attached to either the NH_2 or COOH terminus of the protein without success. We made second generation constructs that contained a polyglycine linker between the fluorescent tag and the TIP47 protein at either end. In all cases, the resulting fusion proteins failed to associate with membranes unlike native TIP47. We will not give up our attempts to generate a functional fluorescent TIP47 protein; we hope to use it to establish whether TIP47 is indeed present on transport vesicles and unlike Rab9 falls off of the vesicles before docking and fusion events. Our working model is that TIP47 collects Rab9 and MPRs into nascent transport vesicles; TIP47 release would then permit Rab9-GTP recruitment of yet to be discovered docking factors that mediate the subsequent events. We hope that future experiments will enable us to test this working model.

Materials and methods

Antibodies and fluorescent protein fusion constructs

Mouse anti–CI-MPR IgG (Lombardi et al., 1993), mouse anti-Rab9 (Soldati et al., 1993), and mouse anti-p115 antibodies (a gift from Gerry Waters, Princeton University, Princeton, NJ) were described previously. Fluorescein-conjugated goat anti–rabbit and Texas red–conjugated goat anti–mouse IgGs were purchased from Jackson ImmunoResearch Laboratories. YFP, GFP, and CFP indicate yellow, green, and cyan fluorescent proteins, respectively, and refer to GFP spectral variants. The parent vectors for pEGFP-C3 (sequence data available from GenBank/EMBL/DDBJ under accession no. U57607), pECFP-C1, pECFP-N1, and pEYFP-C1 were purchased from CLONTECH Laboratories, Inc. The trans-Golgi marker, pECFP-Golgi, encoding CFP fused to the NH_2-terminal region of human β 1,4-galactosyltransferase was purchased from CLONTECH Laboratories, Inc. Rab9 cDNA (Lombardi et al., 1993) and Rab7 cDNA (a gift from Marino Zerial, Max Planck Institute, Dresden, Germany) were cloned at the COOH-terminal end of the GFP and color variants. CD-MPR-CFP represents CFP fused to the COOH terminus of the mouse CD-MPR (a gift from Bernard Hoflack, Institut Pasteur, Lille, France).

Cell culture, antibody uptake, and nocodazole treatment

African green monkey kidney epithelial (BS-C-1) cells were maintained in minimal essential medium supplemented with 7.5% FCS, penicillin, and streptomycin. To visualize endogenous CI-MPRs, cells were washed three times with PBS and incubated for 3 h at 37°C in complete media containing 20 μg/ml Texas red anti–CI-MPR IgG prepared with Texas red sulfonyl chloride according to the manufacturer (2.4 moles Texas red per mole IgG; Molecular Probes). Cells were then chased for 15 min in complete medium; in some experiments, cells were fixed for 15 min in 3% paraformaldehyde before light microscopy. Nocodazole treatment was for 1 h at 37°C in complete medium containing 4 μg/ml nocodazole (Sigma-Aldrich).

Sucrose gradient flotation

BS-C-1 cells were grown on 100-mm plates and transfected with pEGFP-Rab9. After 16–20 h, cells were washed three times with PBS and once

with 10 mM Hepes, pH 7.4. Cells were then swollen for 15 min at 4°C in 10 mM Hepes, pH 7.4, supplemented with protease inhibitors (40 μg/ml aprotinin, 10 μg/ml leupeptin, 1 μM pepstatin A, and 1 μM phenylmethylsulfonyl fluoride). Cells were then harvested by scraping with a rubber policeman in 100 mM KCl, 1.5 mM magnesium acetate, 25 mM Hepes, pH 7.4, supplemented with 1 mM ATP and protease inhibitors. Cell extracts were loaded at the bottom of a nonlinear sucrose gradient (300 μl, 0.5 M sucrose, 300 μl 1.2 M sucrose, and 800 μl 2.5 M sucrose) and centrifuged for 90 min at 54,000 rpm at 4°C in a TLS-55 rotor (Beckman Coulter). Fractions were collected from the top, and equal aliquots were resolved by SDS-PAGE and transferred onto nitrocellulose. Protein distributions were determined by immunoblot using mouse anti-Rab9 culture supernatant (undiluted) and mouse anti-p115 ascites (diluted 1:750).

Live cell imaging and vesicle tracking

Cells grown on glass coverslips were observed 16–20 h after transfection after mounting on a temperature-controlled stage. During observation, cells were maintained in phenol red-free DME containing 7.5% FBS buffered with 20 mM Hepes, pH 7.3, and covered with silicon DC-200 fluid (Serva). Observations were performed on a Nikon Diaphot-300 inverted microscope equipped with a cooled CCD camera (NDE/CCD; Princeton Instruments), and images were analyzed using Metamorph (Universal Imaging Corp.) software. FITC, rhodamine, and dual CFP/YFP filters were from Chroma Technology Corp. Simultaneous detection of CFP and YFP was performed using a dual emission filter by switching between excitation wavelengths with a filter wheel controlled by the Metamorph software. Vesicle motilities were determined at 37°C in cells transfected 16–20 h using the manual tracking point application of Metamorph software and by averaging the distance moved in 10–20 adjacent time intervals.

Immunofluorescence microscopy

Immunofluorescence was performed as described by Warren et al. (1984) using cells grown on glass coverslips. Mouse anti–CI-MPR culture supernatant was used undiluted. Texas red– or fluorescein isothiocyanate-conjugated secondary antibodies were used at 1:1,000.

Online supplemental material

Video 1 shows YFP-Rab9 (red) and CFP-Rab7 (green) in BS-C-1 cells 18 h after transfection. Images were acquired at room temperature to slow intracellular movement. Speed is 14× actual. In video 2, BS-C-1 cells 20 h after transfection with GFP-Rab9 were observed at 37°C. Bidirectional motility along microtubules can be observed (compare with cells treated with nocodazole; video 3). Speed is 5× actual. In video 3, BS-C-1 cells transfected with GFP-Rab9 were treated for 1 h with 4 μg/ml nocodazole. The video shows a Rab9-bearing vesicle budding off of an organelle and fusing with another organelle. Speed is 10× actual. In video 4, BS-C-1 cells 20 h after transfection with YFP-Rab9 (red) and CFP-galactosyltransferase (GalT′ase) (green) were observed at 37°C. The video shows YFP-Rab9–bearing vesicles (arrow) fusing with a CFP-GalT′ase–positive compartment. The video (12× actual speed) contains slowed sequences (3× actual). Videos 1–4 are available at http://www.jcb.org/cgi/content/full/jcb.200109030/DC1.

This research was supported by a grant from the National Institutes of Health (DK37332). P. Barbero was supported in part by the Association pour la Recherche Contre le Cancer; L. Bittova was supported by the Clifford and Evelyn Cherry Fellowship Award of the American Heart Association Western States Affiliate. We extend special thanks to Julie Theriot's lab for assistance with video microscopy, Kate Carroll for help with the color figures, and members of the Pfeffer lab for their critical comments.

Submitted: 10 September 2001
Revised: 2 January 2002
Accepted: 2 January 2002

References

Bucci, C., P. Thomsen, P. Nicoziani, J. McCarthy, and B. van Deurs. 2000. Rab7: a key to lysosome biogenesis. *Mol. Biol. Cell.* 11:467–480.

Carroll, K.S., J. Hanna, I. Simon, J. Krise, P. Barbero, and S.R. Pfeffer. 2001. Role of the Rab9 GTPase in facilitating receptor recruitment by TIP47. *Science.* 292:1373–1377.

Diaz, E., and S.R. Pfeffer. 1998. TIP47: a cargo selection device for mannose 6-phosphate receptor trafficking. *Cell.* 93:433–443.

Diaz, E., F. Schimmöller, and S.R. Pfeffer. 1997. A novel Rab9 effector required for transport from endosomes to the TGN. *J. Cell Biol.* 138:283–290.

Draper, R.K., Y. Goda, F.M. Brodsky, and S.R. Pfeffer. 1990. Anti-clathrin antibodies inhibit endocytosis but not receptor recycling to the *trans* Golgi network in vitro. *Science.* 248:1539–1541.

Duncan, J.R., and S. Kornfeld. 1988. Intracellular movement of two mannose 6-phosphate receptors: return to the Golgi apparatus. *J. Cell Biol.* 106:617–628.

Feng, Y., B. Press, and A. Wandinger-Ness. 1995. Rab 7: an important regulator of late endocytic membrane traffic. *J. Cell Biol.* 131:1435–1452.

Itin, C., C. Rancaño, Y. Nakajima, and S.R. Pfeffer. 1997. A novel assay reveals a role for alpha-SNAP in mannose 6-phosphate receptor transport from endosomes to the TGN. *J. Biol. Chem.* 272:27737–37744.

Itin, C., N. Ulitzur, B. Muhlbauer, and S.R. Pfeffer. 1999. Mapmodulin, cytoplasmic dynein, and microtubules enhance the transport of mannose 6-phosphate receptors from endosomes to the trans Golgi network. *Mol. Biol. Cell.* 10:2191–2197.

Klumperman, J., A. Hille, T. Veenendaal, V. Oorschot, W. Stoorvogel, K. von Figura, and H.J. Geuze. 1993. Differences in the endosomal distributions of the two mannose 6-phosphate receptors. *J. Cell Biol.* 121:997–1010.

Kornfeld, S. 1992. Structure and function of the mannose 6-phosphate/insulin like growth factor II receptors. *Annu. Rev. Biochem.* 61:307–330.

Krise, J.P., P.M. Sincock, J.G. Orsel, and S.R. Pfeffer. 2000. Quantitative analysis of TIP47 (tail-interacting protein of 47kD)-receptor cytoplasmic domain interactions: implications for endosome-to-trans Golgi network trafficking. *J. Biol. Chem.* 275:25188–25193.

Llopis, J., J.M. McCaffery, A. Miyawaki, M.G. Farquhar, and R.Y. Tsien. 1998. Measurement of cytosolic, mitochondrial, and Golgi pH in single living cells with green fluorescent proteins. *Proc. Natl. Acad. Sci. USA.* 95:6803–6808.

Lombardi, D., T. Soldati, M.A. Riederer, Y. Goda, M. Zerial, and S.R. Pfeffer. 1993. Rab9 functions in transport between late endosomes and the trans Golgi network in vitro. *EMBO J.* 12:677–682.

Orsel, J.G., P.M. Sincock, J.P. Krise, and S.R. Pfeffer. 2000. Recognition of the 300K mannose 6-phosphate receptor cytoplasmic domain by TIP47. *Proc. Natl. Acad. Sci. USA.* 97:9047–9051.

Pfeffer, S.R. 1987. The endosomal concentration of a mannose 6-phosphate receptor is unchanged in the absence of ligand synthesis. *J. Cell Biol.* 105:229–234.

Puertollano, R., R.C. Aguilar, I. Gorshkova, R.J. Crouch, and J.S. Bonifacino. 2001. Sorting of mannose 6-phosphate receptors mediated by the GGAs. *Science.* 292:1712–1716.

Riederer, M.A., T. Soldati, A.D. Shapiro, J. Lin, and S.R. Pfeffer. 1994. Lysosome biogenesis requires mannose 6-phosphate receptor recycling from endosomes to the trans-Golgi network. *J. Cell Biol.* 125:573–582.

Sahagian, G.G., and E.F. Neufeld. 1983. Biosynthesis and turnover of the mannose 6-phosphate receptor in cultured Chinese hamster ovary cells. *J. Biol. Chem.* 258:7121–7128.

Soldati, T., M.A. Riederer, and S.R. Pfeffer. 1993. Rad GDI: a solubilizing and recycling factor for Rab9 protein. *Mol. Biol. Cell.* 4:425–434.

Soldati, T., C. Rancaño, H. Geissler, and S.R. Pfeffer. 1995. Rab7 and Rab9 are recruited onto late endosomes by biochemically distinguishable processes. *J. Biol. Chem.* 270:25541–25548.

Sonnichsen, B., S. De Renzis, E. Nielsen, J. Rietdorf, and M. Zerial. 2000. Distinct membrane domains on endosomes in the recycling pathway visualized by multicolor imaging of Rab4, Rab5, and Rab11. *J. Cell Biol.* 149:901–914.

Warren, G., J. Davoust, and A. Cockcroft. 1984. Recycling of transferrin receptors in A431 cells is inhibited during mitosis. *EMBO J.* 3:2217–2225.

Zerial, M., and H. McBride. 2001. Rab proteins as membrane organizers. *Nat. Rev. Mol. Cell Biol.* 72:107–117.